Journal of Thermal Analysis and Calorimetry, Vol. 68 (2002) 231–241

ENERGETIC AND KINETIC EVALUATIONS CONDUCTED IN A QUASI-BINARY Cu–1 AT% Co_2Si ALLOY THROUGH DSC

A. Varschavsky and E. Donoso

Universidad de Chile, Facultad de Ciencias Físicas y Matemáticas, Instituto de Investigaciones y Ensayes de Materiales, IDIEM, Casilla 1420, Santiago, Chile

(Received October 19, 2001)

Abstract

By means of differential scanning calorimetry (DSC) the precipitation process from a supersaturated solid solution of Cu–0.65 at% Co–0.33 at% Si (Cu–1 at% Co_2Si) was investigated. On the basis of enthalpimetric calculations it was found that the decomposition begins with cobalt precipitation. Clustering of atoms of cobalt initiates the precipitation of silicon, and particles of the stoichiometric Co_2Si composition are finally formed. Kinetic parameters were obtained by a convolution method based on the Mehl–Johnson–Avrami formalism. Their values are all in agreement with the experimentally observed behavior displayed by DSC traces. Decay kinetics of cobalt and silicon matrix during simulated isothermal calculations using DSC data reveals good agreement with similar computed results reported in literature. Precipitate dissolution obeys quite well to a three-dimensional diffusion kinetic law previously developed.

Keywords: cobalt, copper, DSC, enegetics, kinetics, precipitation, silicon

Introduction

The development of high strength ternary alloys has been the motive of a series of studies for more than two decades. Most of these alloys fundamented it high mechanical resistance by the formation of extremely fine binary and/or ternary precipitates resistant to be sheared by dislocations, thus giving to the material a high yield stress. In the case of Cu–Co–Si alloys the precipitation process has been studied by electrical resistivity [1–3], thermoelectric power [2, 3] and differential scanning calorimetry [3, 4]. These last studies have justified the mechanical behavior of the alloys and also have given information about the nucleation and growth of the stable precipitates. Co_2Si. Previous authors' works [5, 6] were concerned with the fatigue behavior of some Cu–Co–Si alloys of quasi-binary composition Cu–$x$$Co_2Si$. The principal object of the present work is to evaluate the precipitation process of Co_2Si particles starting from a supersaturated solid solution of Cu–Co–Si utilizing differential scanning calorimetry DSC. An isothermal kinetic calculation of cobalt and silicon matrix decay

1418–2874/2002/ $ 5.00

Akadémiai Kiadó, Budapest
Kluwer Academic Publishers, Dordrecht

during precipitation will also be simulated. Besides two kinetic particles dissolution laws will be tested in order to discriminate the shape of the diffusion field.

Experimental

The alloy utilized was prepared in vacuum in a Baltzers VSG-10 induction furnace, from electrolytic copper (99.95% purity), and master alloys of Cu–10 mass% Co and Cu–15 mass% Si. After chemical analysis it was found that the alloy contained Cu–0.65 at% Co-0.33 at% Si (Cu–1 at% Co_2Si). The ingot was forged at 1273 K to a thickness of 20 mm, afterwards it was annealed at 1273 K during 72 h to achieve complete homogenized and furnace-cooled to room temperature. Subsequently, the material was cold-rolled to a thickness of 2 mm with intermediate annealings of 1 h at 1273 K.

After the last anneal the alloy was water quenched. Calorimetric measurements were carried out in a DuPont 2000 thermal analyser at heating rates (ϕ) of 0.03, 0.08, 0.17, 0.33 and 0.83 K s^{-1}. To increase the sensitivity of the measurements, high purity, well annealed copper disc, was used as a reference. In order to minimize oxidation dried nitrogen ($0.8 \cdot 10^{-4}$ m^3 min^{-1}) was passed through calorimeter.

Runs were recorded between 300 and 950 K. After the first run each specimen was maintained at 850 K for 5 min and allowed to cool freely in the calorimeter for 3 h yielding cooling curves that were very similar and nearly exponential. It was observed that the cooling rate was 0.417 K s^{-1} at 850 K, and 0.117 K s^{-1} below 560 K. When room temperature was reached, a second run at the same heating rate was made by heating each specimen up to 850 in order to avoid displayement of the Co_2Si dissolution reaction. DSC traces presented in this work were obtained by subtracting the baseline from the first run. This baseline represents the temperature-dependent heat capacity of the alloy in the existing thermal conditions, and its value was in agreement with the Kopp–Neumann rule. Afterwards, the resulting traces were converted into a differential heat capacity *vs*. temperature curve. The heat-capacity remainder, namely the differential heat capacity ΔC_p represents the heat associated with solid state reactions during the DSC run. Thus, reaction peaks in ΔC_p *vs. T* curve can be characterized by the reaction enthalpy of a particular event. DSC curves presented in this work are all such rerun-corrected curves.

Results and discussion

Energetics

Figure 1 shows typical curves for the Cu–1 at% Co_2Si alloy in the form of differential heat capacity (ΔC_p) *vs*. temperature for different heating rates ϕ. In DSC curves at low and medium heating rates scanned, two successive exothermic semi-overlapped peaks stages 1 and 2 and one endothermic peak, stage 3 are displayed. It is the aim of this section to explore via enthalpimetric methods the nature of each of such peaks.

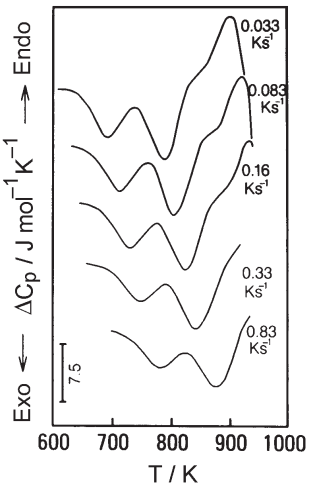

Fig. 1 DSC traces for quenched Cu–1 at% Co_2Si alloy. Heating rates and the three main effects are shown

Firstly, the area of the heat evolved in the exothermic peaks ΔH_1 and ΔH_2 are computed. The corresponding experimental results (areas under ΔC_p *vs*. *T* curves) are plotted in Fig. 2. Curve (d) for stage 1 and (b) for stage 2. If we assume that stage 1 can be attributed to Co precipitation, its molar heat of precipitation should be first estimated. In absence of specific data we perform this computation using the solubility

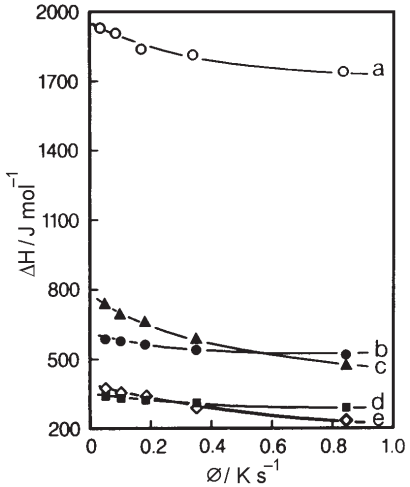

Fig. 2 Heat contents of stages 1 and 2 for quenched Cu–1 at% Co_2Si alloy. a – calculated heat content $\Delta H_c^{Co_2Si}$ for precipitation of Co_2Si in stage 2; b – experimental heat content $\Delta H_2=\Delta H_e^{Co_2Si}$ measured in stage 2; c – calculated heat content $\Delta H_c^{Co-Co_2Si}$ for the transition of stage 2; d – experimental heat content for precipitation of Co in stage 1 $\Delta H_1=\Delta_e^{Co}$ and e – calculated heat content ΔH_c^{Co} for precipitation of Co in stage 1

curve of Servi and Turnbull [7] for the Cu–Co binary system as a first approximation. It is believed that the presence of Si shifts this curve to the left, thus accelerating the precipitation of Co [3]. In this solubility curve, taking two alloy compositions c_1=0.01 and c_2=0.002 the corresponding solubility temperatures were found to be T_1=1010 K and T_2=854.7 K. By employing van't Hoff isochore, the molar heat of precipitation for Co in Cu, ΔH_p^{Co} can be estimated from

$$\ln\left(\frac{\bar{c}_1}{\bar{c}_2}\right)=\left(\frac{1}{T_2}-\frac{1}{T_1}\right)\frac{\Delta H_p^{Co}}{R} \tag{1}$$

giving ΔH_p^{Co}=74.4 kJ mol^{-1}. Hence, the calculated heat of precipitation ΔH_c^{Co} corresponding to stage 1 might be obtained as [8, 9]:

$$\Delta H_c^{Co}=\Delta H_p^{Co}\left[\bar{c}_{Co}-c_M^{Co}\left(T_{e1}\right)\right] \tag{2}$$

where $\bar{c}_{Co}$ is the cobalt alloy composition and $c_M\left(T_{e1}\right)$ is the matrix composition at the ending temperature of stage 1 T_{e1}, also obtained from Servi and Turnbull solubility curve. Calculated ΔH_c^{Co} values were plot *vs*. the heating rates in Fig. 2e. If such values are compared with the experimental ones $\Delta H_1=\Delta H_c^{Co}$ of Fig. 2d, it can be seen a fairly good fitting between both curves, thus confirming that stage 1 is due to Co precipitation. By repeating the same procedure with stage 2, in order to search if this stage can be attributed to Co_2Si precipitation, the molar heat precipitation of Co_2Si, $\Delta H_p^{Co_2Si}$ can be estimated from the solubility curve of Albert [1]. According to the thermodynamics of ternary systems [10] the compositions c_{Co} and c_{Si} dissolved can be written as

$$c_{Co}^2 c_{Si}\approx\exp\left(-\frac{\Delta H_p^{Co_2Si}}{RT}\right) \tag{3}$$

and

$$c_{Co}^2 c_{Si}\approx c_{Co_2Si}^3 \tag{4}$$

thus:

$$c_{Co_2Si}=\exp\left(-\frac{\Delta H_p^{Co_2Si}}{3RT}\right) \tag{5}$$

and again by using van't Hoff isochore:

$$\ln\left(\frac{\bar{c}_1}{\bar{c}_2}\right)=\left(\frac{1}{T_2}-\frac{1}{T_1}\right)\frac{\Delta H_p^{Co_2Si}}{3R} \tag{6}$$

By employing values for $c_{Co,Si}$ of $\bar{c}_1$=0.01 and $\bar{c}_2$=0.005, from Albert's solubility curve the dissolution temperatures found were T_1=1165 K and T_2=1068 K. After computations one gets $\Delta H_p^{Co_2Si}$=221.62 kJ mol^{-1}. If now stage 2 is attributed to direct

Co_2Si precipitation, application of an equation similar to Eq. (2) for Co precipitation, leads to the curve appearing in Fig. 2a for T_{e2}, the ending temperatures of stage 2. It then must be concluded that stage 2 cannot be attributed to direct Co_2Si precipitation. Instead, if one assumes that stage 2 corresponds to a calculated transition $\Delta H_c^{Co-Co_2Si}$ from stage 1 as follows [8, 9]:

$$\Delta H_c^{Co-Co_2Si} = (\Delta H_p^{Co_2Si} - \Delta H_p^{Co}) \left[c_{Co} - c_M^{Co}(T_{e1}) \right] \quad (7)$$

and their values are plotted *vs*. ϕ, the curve of Fig. 2c results. It is then inferred that stage 2 with its associated heat $\Delta H_2 = \Delta H_e^{Co_2Si}$ is then formed by diffusion of Si in Co leading to a transition. Regarding stage 3, the enthalpimetric computed values ΔH_3 are in very good agreement with those of stage 2 ΔH_2, leading to the conclusion that it corresponds to Co_2Si particles dissolution. For instance, the heats evolved in stage 2 for ϕ=0.033 and 0.083 K s^{-1} are 585 and 577 J mol^{-1}, while for the same heating rates the endothermic heats associated with stage 3 yield 580 and 570 J mol^{-1}. The nature of stages 1 and 2 are in good agreement with those interpretations previously arising from thermoelectric power and resistivity measurements [1–3].

Precipitation kinetics

To study the precipitation kinetics of the present reactions thoroughly, activation energies E were calculated by a modified Kissinger method [11]

$$\ln\left(\frac{T_p^2}{\phi}\right) = \frac{E}{RT_p} + \ln\left(\frac{E}{Rk_0}\right) \quad (8)$$

where T_p is the peak temperature, k_0 a pre-exponential constant and R the gas constant. Therefore, E and also k_0 can be obtained from the plot $\ln(T_p^2/\phi)$ *vs*. $1/T_p$. These curves are shown in Fig. 3 where the straight lines are distinguished for the three stages. In Table 1 one can read the respective values of the activation energies and pre-exponential factors. It can be inferred that the values of activation energies resulted somewhat larger than those reported by Lendvai *et al*. [3]. Utilizing Brown and

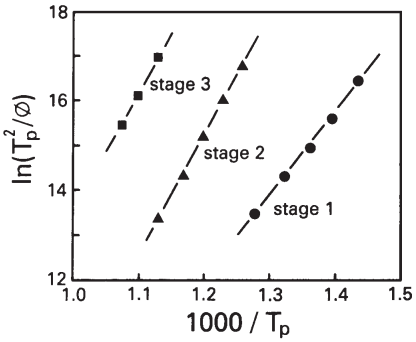

Fig. 3 Modified Kissinger plots for the different DSC stages in a quenched Cu–1 at% Co_2Si alloy

Ashby [12] and also Shi *et al*. [13] correlations, the activation energy for diffusion of Co in Cu, E_{Cu}^{Co}=164.5 kJ mol^{-1} and Si in Co, E_{Co}^{Si}=227.1 kJ mol^{-1} were estimated, resulting fairly consistent with those obtained by the modified Kissinger method for stages 1 and 2. For stage 3, the activation energy lies between the activation the energy for diffusion of Si in Cu E_{Cu}^{Si}=199.8 kJ mol^{-1} and that for Co in Cu, as can be expected from the dissolution process of Co_2Si particles in the Cu matrix.

Table 1 Values of activation energies and pre-exponential factors

	Stage 1	Stage 2	Stage 3
E/kJ mol^{-1}	155.6	220.5	215.6
k_0/s^{-1}	$6.6\cdot10^{8}$	$4.3\cdot10^{11}$	$6.5\cdot10^{9}$

The kinetic analysis was performed according to Johnson–Mehl–Avrami equation usually used for heterogeneous reactions (as there are in the present case) under non-isothermal conditions

$$y=1-\exp\left[-(k_0\theta)^n\right] \tag{9}$$

where y is the reacted fraction, k_0 a pre-exponential factor,

$$\theta=\frac{T^2R}{\phi E}\exp\left(-\frac{E}{RT}\right) \tag{10}$$

is the reduced time [14, 15], and n a constant.

If two DSC peaks overlap each other, such is the situation for Co and Co_2Si formation, the total heat flow $\Delta\dot{H}_T$ per unit mass at any time/temperature can be expressed as the sum of the heat flow of the individual transformations $\Delta\dot{H}_1$ and $\Delta\dot{H}_2$ as [16]:

$$\Delta\dot{H}_T=\Delta\dot{H}_1+\Delta\dot{H}_2=A_1\dot{y}_1+A_2\dot{y}_2 \tag{11}$$

In this equation A_1 and A_2 are the areas of the individual peaks, while $\dot{y}_1$ and $\dot{y}_2$ are the transformation rates, being easily derived for each reaction from Eq. (5) as:

$$\left(\frac{dy}{dt}\right)=nk_0^n\theta^{n-1}\frac{d\theta}{dt}\exp\left[-(k_0\theta)^n\right]$$

which with the aid of Eq. (10) becomes:

$$\dot{y}=nk_0^n\left(\frac{T^2R}{\phi E}\right)^{n-1}\exp\left(-\frac{nE}{RT}\right)\exp\left[-k_0^n\left(\frac{T^2R}{\phi E}\right)^n\exp\left(-\frac{nE}{RT}\right)\right] \tag{12}$$

From Eq. (11), after assigning to reactions 1 and 2 the respective subscripts, one finally obtain

$$\dot{H}_T = \sum_{i=1}^{2} A_i n_i k_{0_i}^{n} \left(\frac{T^2 R}{\phi E_i} \right)^{n_i - 1} \exp\left(-\frac{n_i E_i}{RT} \right) \exp\left\{ -\left[\left(\frac{T^2 R}{\phi E_i} \right)^{n_i} k_0^{n_i} \exp\left(-\frac{n_i E_i}{RT} \right) \right] \right\} \quad (13)$$

The area of the individual peaks must add up the total area $A=A_1+A_2$. This equation is identical to that obtained previously by Borrego and González-Docel [17, 18] working with $k_0\phi$ as a state variable. By fitting this equation to the experimental heat flow data $\Delta\dot{H}_T$ employing computerized methods of minimization of least squares error, the parameters n_1=1.13 and n_2=1.48 can be obtained, which in conjunction with the apparent activation energies E_1 and E_2 and the pre-exponential factors calculated from the modified Kissinger method constitute the kinetic parameters for each individual reaction. Also parameters A_1 and A_2 can be calculated and hence, since heat flow per unit mass of the sample $\Delta\dot{H}=\Delta C_p\phi/MW_s$ where MW_s is the molecular mass of the precipitate, the associated reaction heat can be readily obtained. The respective values obtained are ΔH_1=325 J mol^{-1} and ΔH_2=563 J mol^{-1}. Fitting of the calculated to the experimental curve is shown in Fig. 4 for ϕ=0.17 K s^{-1}. In this figure the experimental curve, the adjusted curve and the individual curves corresponding to each stage are shown. These values are in fairly good accordance with those obtained from the energetics of both processes.

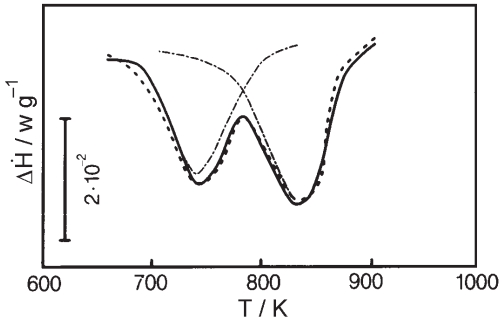

Fig. 4 Heat flow *vs*. temperature from DSC experiments at ϕ=0.167 K s^{-1}. — experimental composite curve; - - - calculated composite curve; – · – approximation to individual stages 1 and 2

The value of n_1 is closely indicative of a process of nucleation and growth (n=1) while that for n_2 is nearly indicative of a process of growth from pre-existing nucleus of non-negligible size (n=1.5) [19].

As an alternative model to visualize the process of precipitation of Co followed by Si diffusion into cobalt particles to form Co_2Si precipitates, an isothermal simulation will be made using kinetic data obtained by DSC. In this simulation the kinetics of decay content of Co and Si in the matrix will evaluated. In order to perform it the reacted fractions for Co and Si involved in the transition to Co_2Si can be defined as

$$y_{Co} = \frac{V^{Co}}{V_e^{Co}} \text{ and } y_{Si} = \frac{V^{Si}}{V_e^{Si}} \quad (14)$$

where V^{Co}, V^{Si} are the instantaneous volume fractions and V_e^{Co}, V_e^{Si} are the Co and Si equilibrium volume fractions belonging to the Co_2Si precipitates at temperature T. As in general the volume fraction for any particle is given by $V=(\bar{c}-c_M)/(c_p-c_M)$, being $\bar{c}$ the alloy concentration, c_p the precipitate and c_M the matrix concentrations, one has for Co_2Si in equilibrium:

$$V_f^{Co_2Si}=\frac{\bar{c}^{Co_2Si}-c_M^{Co_2Si}}{c_p^{Co_2Si}-c_M^{Co_2Si}} \tag{15}$$

where $c_M^{Co_2Si}$ is obtained from the solubility curve of Albert [1] at temperature T considered, $\bar{c}^{Co_2Si}=0.01$ and $c_p^{Co_2Si}=1$. Now, we assume that Co and Si shares the volume fraction of Co_2Si in the same proportion that in the unit cell. Hence $V_e^{Co}=2/3V_e^{Co_2Si}$ and $V_e^{Si}=1/3V_e^{Co_2Si}$. This assumption might be justified since the atomic diameters d, of Co and Si are very similar ($d^{Co}=0.25$ nm and $d^{Si}=0.236$ nm) and further corroborated from calculated values using Albert's solubility curve [1] for computation of $2/3Co_2Si$ and that from Servi and Turnbull [7] for Co at 650 and 730 K. For $2/3Co_2Si$, volume fractions of 0.0059 and 0.0053 respectively were obtained, while for Co, values of 0.0052 and 0.0048 were measured, thus showing a fairly good agreement. Therefore, by using Eq. (4) and the function which relates V to c_M given before, for each atomic isolated species considered it holds:

$$c_M^{Co}=\frac{\bar{c}^{Co}-y_{Co}c_p^{Co}V_e^{Co}}{1-y_{Co}V_e^{Co}} \tag{16}$$

and

$$c_M^{Si}=\frac{\bar{c}^{Si}-y_{Si}c_p^{Si}V_e^{Si}}{1-y_{Si}V_e^{Si}} \tag{17}$$

where $\bar{c}^{Co}=0.0065$ and $\bar{c}^{Si}=0.0033$ (the atomic fractions contained in the alloy). In Eqs (16) and (17) $c_p^{Co}=1$ and $c_p^{Si}=1$, as Co and Si atoms are considered separately. By invoking the transferability principle, that is, kinetic parameters calculated in non-isothermal and isothermal experiments are the same, y_{Co} can be taken as the one corresponding to the first Co precipitation peak, while y_{Si} to the values associated with the transition to Co_2Si, where Si atoms diffuse into cobalt precursor particles, namely the second heat effect.

Results for the matrix Co and Si concentration decay are shown in Figs 5 and 6 taken $y_1=y_{Co}$ and $y_2=y_{Si}$ from DSC data at 650 and 730 K. At 650 K, Co decay in a great extent while Si concentration remains essentially the same. Also it can be observed in Fig. 5 the rapid Co decay at 730 K, thus showing that DSC and the isothermal computations are complementary each other. On the other hand, these results are identical to those obtained experimentally by Albert [1] using electric resistivity measurements. In this way energetic and kinetic calculations arising from DSC experiments show perfect accordance with those obtained isothermally by electrical resistivity methods.

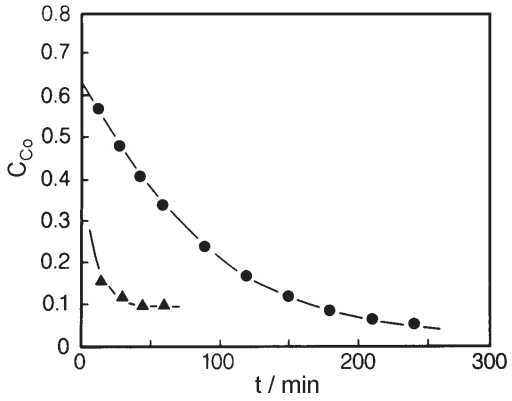

Fig. 5 Isothermal simulated Co concentration decay *vs*. time curves ● – 650 K, ▲– 730 K

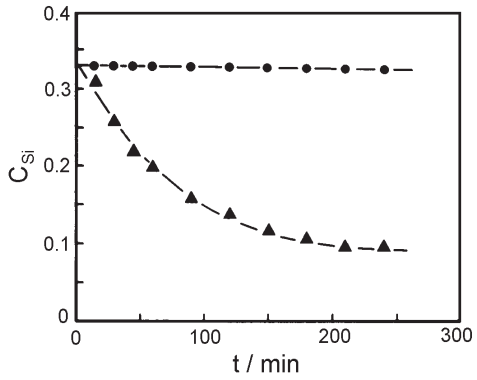

Fig. 6 Isothermal simulated Si concentration decay *vs*. time curves ● – 650 K, ▲– 730 K

Precipitate dissolution

The kinetic analysis for stage 3 was performed on the basis of a non-isothermal precipitate dissolution kinetic approach already discussed in early papers [20, 21]. In such an approach three-dimensional controlled situations are essentially described by means of the expression

$$1-(1-y)^{2/3}=k_1\theta \tag{18}$$

while one-dimensional diffusion situations are better described by means of

$$[1-(1-y)^{1/3}]^2=k_2\theta \tag{19}$$

where k_1 and k_2 are constants and θ is already defined. In the values of θ the activation energy of stage 3 was considered. The results of plotting *vs*. θ the left-hand side terms of Eqs (18) and (19), called integrated kinetic functions $F(y)$, are shown in Fig. 7. It is clearly seen in this figure that the dissolution behaviour of Co_2Si is adjusted to the

model suitable for a curved interface and a three-dimensional diffusion situation, which is consistent with spherical-like precipitates [3].

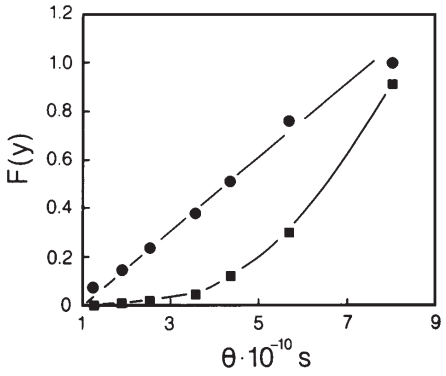

Fig. 7 Plots of two integrated kinetic functions *vs*. θ. ● – Eq. (18), ■ – Eq. (19) ϕ=0.083 K s^{-1}

Finally, it is worth noticing the rather skewed shape of the dissolution peak during DSC run in Fig. 1. The slow reaction rate at the early stages can be attributed to the combined effects of a slow diffusion rate, because at low heating rates the temperature is not high enough, the small concentration gradient near the particle-matrix interface and the relatively small interfacial area to particle volume dissolution rate. The dissolution rate is increasing with the temperature rising and towards the end of the dissolution process the rate is very high. This is because the combined effect of a high diffusion rate, the large concentration gradient near the interface and the expected high ratio of interface area to particle volume. It is also expected that the particle size affects the kinetics of dissolution. Small particles should tend to shift the peak to smaller temperatures and to be fully dissolved in a shorter time, while increasing particle radius shift the peak to higher temperatures. A small particle size may correspond to a high particle density for a fixed volume fraction of particles, so the diffusion distances are smaller and the reaction reaches completion faster than for a small particle density. These subjects are under study for a next work.

Conclusions

In the Cu–1 at% Co_2Si alloy investigated the precipitation process of the supersaturated solid solution obtained by solution treatment and quenching starts with the precipitation of Co atoms as shown by differential scanning calorimetry performed in the present work, followed by a transition reaction leading to Co_2Si precipitate formation. It could be thus constated that Co precipitates grow more rapidly than Co_2Si ones being the precursors of their formation. The kinetic parameters for Co and Co_2Si formation determined from equations based in the Mehl–Johnson–Avrami formalism were consistent with the precipitation sequence. Simulated Co and Si matrix decay

concentrations during isothermal precipitation are in good agreement with reported literature results. Finally, precipitate dissolution kinetics can be described by a three-dimensional diffusion controlled model.

* * *

The authors wish to acknowledge the Fondo de Desarrollo Cientifico y Tecnológico (FONDECYT), Project 1980731 and the Instituto de Investigaciones y Ensayes de Materiales, Facultad de Ciencias Físicas y Matemáticas, Universidad de Chile for the facilities provided for this research.

References

1 B. Albert, Z. Metallk., 75 (1985) 475.
2 B. Albert, Z. Metallk., 75 (1985) 528.
3 J. Lendvai, T. Ungar, I. Kovács and B. Albert, J. Mater. Sci., 23 (1988) 4059.
4 E. Donoso and A. Varschavsky, Anales del 49º Congreso Internacional de Tecnología de Materiales y III Congreso Iberoamericano de Ingeniería Metalúrgica y de Materiales, Octubre 1994, Sao Paulo, Brasil, Vol. II, p. 493.
5 A. Varschavsky and E. Donoso, Mater. Letts., 15 (1992) 207.
6 A. Varschavsky and E. Donoso, Anales del III Congreso Iberoamericano de Ingeniaría Mecánica, Septiembre 1997, La Habana, Cuba, Vol. I, p. 119.
7 I. S. Servi and D. T. Turnbull, Acta Metall., 14 (1966) 161.
8 J. M. Strarnik and P. Van Mourik, Metall. Trans., 22A (1991) 665.
9 A. Varschavsky and E. Donoso, Thermochim. Acta, 266 (1995) 665.
10 R. H. Parker, An Introduction to Chemical Metallurgy, Pergamon Press, Oxford 1978, p. 38.
11 E. J. Mittemeijer, Lui Cheng, P. J. Van der Shaaf, C. M. Brakman and B. M. Korevaar, Metall. Trans., 19A (1988) 925.
12 A. M. Brown and M. F. Ashby, Acta Metall., 28 (1980) 1085.
13 F. J. Shi, T. G. Nieh and Y. T. Chou, Scripta Mater., 43 (2000) 265.
14 A. Varschavsky, Thermochim. Acta, 203 (1992) 391.
15 A. Varschavsky and J. Šesták, Characterization Techniques of Glasses and Ceramics, J. M. Rincón and M. Romero, Eds Springer, New York 1999, p. 85.
16 R. F. Skeyer, B. C. Richardson and S. H. Risbud, Metall. Trans., 17A (1986) 1479.
17 A. Borrego and G. González-Docel, Mater. Sci. Eng., A245 (1998) 10.
18 A. Borrego and G. González-Docel, Mater. Sci. Eng., A276 (2000) 292.
19 J. W. Christian, The Theory of Transformation of Metals and Alloys, 2º Ed., Pergamon Press, England 1971, p. 534.
20 A. Varschavsky and E. Donoso, Thermochim. Acta, 69 (1983) 341.
21 A. Varschavsky and E. Donoso, J. Mater. Sci., 21 (1986) 3873.